American Mineralogist, Volume 63, pages 535–543, 1978

Crystal chemistry of titanian chondrodite and titanian clinohumite of high-pressure origin[1]

KIYOSHI FUJINO[2] AND YOSHIO TAKÉUCHI

Mineralogical Institute, Faculty of Science
University of Tokyo, Hongo, Tokyo 113, Japan

Abstract

The crystal structures of titanian chondrodite [$Mg_{3.99}Fe_{0.57}Mn_{0.01}Ni_{0.01}Ti_{0.42}(SiO_4)_2OH_{1.15}O_{0.85}$; a = 4.7271(7), b = 10.318(1), c = 7.9053(9)A, α = 109.333(8)°, $P2_1/b$, Z = 2] and titanian clinohumite [$Mg_{7.44}Fe_{1.09}Mn_{0.02}Ni_{0.02}Ti_{0.43}(SiO_4)_4OH_{1.14}O_{0.86}$; a = 4.745(1), b = 10.283(2), c = 13.699(3)A, α = 101.00(2)°, $P2_1/b$, Z = 2] from the Buell Park (Arizona) kimberlite have been refined by full-matrix least-squares methods to R = 0.035 and 0.026, respectively. The results have established that Ti in the both structures is exclusively concentrated in the $M(3)$ site located in Mg(OH)O layers. This situation explains the fact that attainable substitution of Ti for Mg in chondrodite is higher than that in clinohumite.

The final difference Fourier synthesis of titanian clinohumite has brought out hydrogen positions, H and H′, which are related to each other by inversion, the separation between H and H′ being 0.87A, and O–H = 1.02A. This feature implies that if the positions were fully occupied by hydrogen atoms as in the OH end-member, there would arise a strong hydrogen–hydrogen repulsion. The substitution, Mg + 2(OH) → Ti + 2(O), that reduces the number of OH groups in the structure, would therefore play a role in reducing the effect of repulsion to stabilize the structure, thus explaining the non-occurrence in nature of OH end-members of the humite-group minerals; the substitution of F for OH would then play the same role.

Introduction

The minerals of the humite group are known so far to occur typically in metamorphosed and metasomatised limestones and dolomites and in skarns associated with ore deposits at contacts with acid plutonic rocks. Recently, McGetchin *et al.* (1970) pointed out that titanian clinohumite in the Moses Rock kimberlite had possibly equilibrated in the upper mantle at depths ranging from about 50 to 150 km at modest temperatures, generally less than 1000°C.

In experimental investigations under high pressure of the system MgO–SiO_2–H_2O, Yamamoto and Akimoto (1974, 1977) synthesized crystals of hydroxyl–clinohumite and –chondrodite at pressures between 29 and 77 kbar and temperatures between 700 and 1200°C. This suggested that clinohumite and chondrodite might be stable between 70 and 120 km depth in the upper mantle, and in fact Aoki *et al.* (1976) discovered titanian chondrodite and clinohumite in the Buell Park (Arizona) kimberlite, and gave a detailed account of the petrological significance of these minerals.

The present paper is a crystallographic counterpart of the investigation of these high-Ti minerals. Robinson *et al.* (1973) suggested a random distribution of Ti among octahedral positions, whereas Kocman and Rucklidge (1973) found Ti exclusively concentrated in the "Mg(OH,F)O layers", the notation of which was initiated by Ribbe *et al.* (1968) to substitute for "$Mg(OH,F)_2$ layers" in the humite group minerals. Our materials are suited to resolve this conflict because of their high Ti contents.

Material

Crystals of titanian chondrodite and clinohumite (abbreviated Ti–Ch and Ti–Cl, respectively) used in our study were collected from the heavy-mineral con-

[1] According to the suggestion made by Dr. A. Kato, chairman, Commission on New Minerals and Mineral Names, National Science Museum, Tokyo, Japan and Dr. C. A. Francis, Department of Geological Sciences, Virginia Polytechnic Institute and State University, we use in this paper the terminology titanian chondrodite and titanian clinohumite instead of titanochondrodite and titanoclinohumite to express Ti-bearing chondrodite and clinohumite respectively.

[2] Present address: Department of Earth Sciences, Ehime University, Bunkyo-cho, Matsuyama 790, Japan.

0003–004X/78/0506–0535$02.00

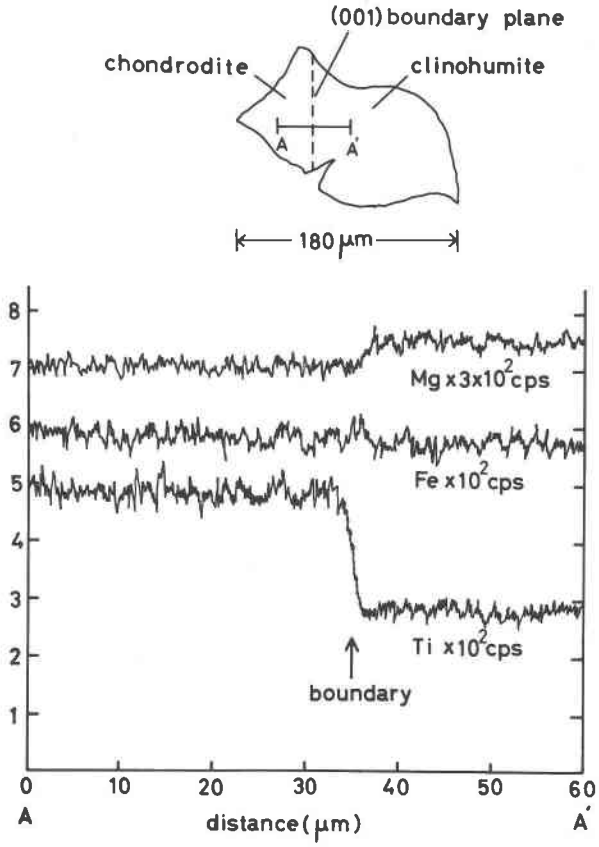

Fig. 1. Microprobe traverse across the boundary of the epitaxial intergrowth of titanian chondrodite and clinohumite in a single grain.

centrates placed at our disposal by Professor Aoki. Since refractive indices of Ti-Ch and Ti-Cl are α = 1.714, 1.686, β = 1.717, 1.695 and γ = *ca.* 1.750, 1.720, respectively (Aoki *et al.*, 1976), it is difficult to distinguish one from the other by the optical properties only.

Chemical compositions of a number of chondrodite and clinohumite crystals of the Aoki specimens are summarized in Table 1 of Aoki *et al.* (1976). Microprobe analyses of Ti-Ch and Ti-Cl crystals used for our structure analyses are listed in Table 1 of this paper. As will be observed in these tables, the specimens may be classified into two groups on the basis of their TiO_2 content: those in the first group range from 7.3 to 10.2 weight percent TiO_2 and those in the second 3.6 to 5.7 weight percent. X-ray precession photographs have shown that the specimens of the first group are exclusively chondrodites and those of the second clinohumites. Our chondrodite thus contains significantly more Ti than clinohumite, and this is in contrast to the report of Jones *et al.* (1969) that the amount of Ti substitution for Mg appears to increase from norbergite to clinohumite. Our result, however, confirms the validity of the general formula, $nM_2SiO_4 \cdot M_{1-x}Ti_x(OH,F)_{2-2x}O_{2x}$ where M = Mg + Fe + Mn + Ca + Zn $\cdots$ and $x < 1$, which was given to the humite-group minerals based on the proposed substitution scheme, M + 2(OH,F) $\rightleftarrows$ Ti + 2(O) (Jones *et al.*, 1969).

Neither the Ti-Ch nor the Ti-Cl specimens showed detectable fluorine content in electron microprobe analyses.

Several specimens contained both chondrodite and clinohumite in a single grain. They showed epitaxial intergrowths of both minerals with their a and b axes in common. If $100x|a - a'|/\frac{1}{2}(a + a')$ and $100x|b - b'|/\frac{1}{2}(b + b')$ are defined as measures of misfit across (100), where a, b and a', b' are the lattice parameters of clinohumite and chondrodite, respectively, we found that these values were very small; *e.g.* for one specimen they were 0.4 percent and 0.3 percent respectively. A microprobe traverse between the two minerals (Fig. 1) showed that the Ti content was discontinuous at the boundary, whereas other contents had approximately the same values across the boundary. It should be noted that no trace of humite, which is the intermediate member in composition between chondrodite and clinohumite in the humite-group minerals, was observed at the boundary. A

Table 1. Chemical compositions and unit-cell parameters of titanian chondrodite and clinohumite used for structure analyses

Microprobe analyses	Ti-Ch (wt.%)	Ti-Cl (wt.%)	Unit cells	Ti-Ch	Ti-Cl
SiO_2	32.54	35.06	a(Å)	4.7271(7)	4.745(1)
TiO_2	9.36	5.07	b(Å)	10.318(1)	10.283(2)
Al_2O_3	0.01	0.05	c(Å)	7.9053(9)	13.699(3)
Cr_2O_3	0.04	0.06	α(°)	109.333(8)	101.00(2)
FeO	11.27	11.56	V(Å^3)	363.82(8)	656.04(23)
MnO	0.22	0.24	Space group	$P2_1/b$	$P2_1/b$
MgO	44.47	44.35	Z	2	2
NiO	0.20	0.20			
CaO	n.d.	0.01			
H_2O(calc.)*	2.76	1.48			
Total	100.86	98.08			

Chemical formula used in refinement

Ti-Chondrodite

$Mg_{3.989}Fe_{0.567}Mn_{0.011}Ni_{0.010}Ti_{0.424}(SiO_4)_2OH_{1.152}O_{0.848}$

Ti-Clinohumite

$Mg_{7.437}Fe_{1.088}Mn_{0.023}Ni_{0.018}Cr_{0.005}Ti_{0.429}(SiO_4)_4OH_{1.142}O_{0.858}$

**Calculated from theoretical formula of Jones et al. (1969).*
n.d. = not determined.
The error in the final figure is indicated in parentheses.

Table 2. Unit-cell parameters of selected chondrodites and clinohumites

	TiO_2 wt.%	a (Å)	b (Å)	c (Å)	α (°)	V (Å^3)
Ch(present work)	10.19	4.73	10.34	7.91	109.5	365.0
" (")	7.32	4.72	10.30	7.89	109.3	362.7
Cl(")	5.68	4.74	10.28	13.69	101.0	654.2
" (")	3.60	4.74	10.26	13.68	101.0	652.4
Ch(Jones et al., 1969)	0.47	4.7332	10.2552	7.8765	109.128	361.22
Cl(")	0.22	4.7441(2)	10.2501(5)	13.6635(3)	100.786(2)	652.68
" (")	5.59	4.7451(8)	10.288(2)	13.691(1)	100.657(8)	656.83
Ch(Yamamoto et al., 1974)	0.00	4.752(1)	10.350(2)	7.914(2)	108.71(5)	368.7(1)
Cl(Yamamoto et al., 1977)	0.00	4.7474(2)	10.284(1)	13.695(1)	100.64(1)	657.1(1)

Ch = chondrodite, Cl = clinohumite.
The error in the final figure is indicated in parentheses.

salient feature of the chemical analyses of both phases in such a paired specimen is that the Ti/Si ratio in the chondrodite phase is exactly twice as great as that in the other phase, clinohumite (refer to Table 2 in Aoki *et al.*, 1976). This fact strongly suggests the preferential distribution of Ti ions into the regions of the Mg(OH)O layers in the crystal structures of chondrodite and clinohumite. This is, in fact, confirmed by the crystal-structure analyses, as will be discussed later.

Unit cell

The cell dimensions of Ti–Ch and Ti–Cl used for our structure analyses, obtained by single-crystal diffractometry, are listed in Table 1 with their chemical compositions. Cell parameters of the specimens with maximum and minimum TiO_2 contents were determined with the precession method, and they are listed in Table 2, together with those of the other investigators. Our values in the table are slightly different from corresponding ones previously reported (Aoki *et al.*, 1976), because we have now introduced a new correction factor for film shrinkage based on cell dimensions obtained from single-crystal diffractometry; the present values are more reliable than previous ones. The space group $P2_1/b$ (unique axis a) is adopted because it permits direct comparison with the olivines and other humite-group minerals (Jones, 1969).

In Table 2 there seems to be a slight increase in cell parameters, especially b axis, with increase in Ti content of natural Ti–Ch and Ti–Cl. This is rather an unexpected result when we compare the ionic radii of Mg^{2+} and Ti^{4+} (Mg^{2+} = 0.720A, Ti^{4+} = 0.605A; Shannon and Prewitt, 1969). It may partly be due to the incorporation of Fe into the structure (Jones *et al.*, 1969, Fig. 1).

Other characteristics observed in the X-ray precession photographs are the frequent occurrence of (100) twins in chondrodite. In thin sections under the microscope most of these twins were ascertained to be polysynthetic. Moreover, the frequency of the twins appears to depend on the Ti content of the crystals. Chondrodite specimens having TiO_2 contents higher than about 9.5 weight percent showed (100) twins without exception. Such a close relation between the twin occurrence and Ti contents of the crystals will be reported elsewhere, together with a suggested mechanism for twinning.

Refinement of the structures

Intensity data collection

Twin-free single crystals of Ti–Ch and Ti–Cl were used for structure analyses. Intensity data were collected in the range $2\theta < 80°$ (Mo$K\alpha$) for Ti–Ch and $2\theta < 65°$ for Ti–Cl on an automated four-circle diffractometer SYNTEX $P2_1$. Only reflections with intensities greater than $3\sigma(I_0)$ were used for structure refinements (1329 for Ti–Ch; 1746 for Ti–Cl). After correcting for Lorentz and polarization the sets of intensities were reduced to structure amplitudes. An absorption correction was made for Ti–Cl (μ = 24.2 cm^{-1}), but not for Ti–Ch. Information about intensity data collection is summarized in Table 3 with the refined extinction parameters and R-values.

Refinement procedure

Full-matrix least-squares refinements were carried out using the program LINUS (Coppens and Hamilton, 1970). The positional parameters of chondrodite (Gibbs *et al.*, 1970) and those of clinohumite (Robinson, *et al.*, 1973) were used as initial parameters

Table 3. Information about intensity data collection with refined extinction parameter and *R*-value

	Ti-Chondrodite	Ti-Clinohumite
Crystal size (mm)	0.09x0.10x0.14	ϕ=0.16
Linear absorption coefficient (cm^{-1})	25.8	24.2
$2\theta_{max.}$	80.0°	65.0°
No. of indep. reflections measured	1623	2322
No. of indep. reflections used for refinement with $I_o > 3\sigma(I_o)$	1329	1746
Extinction coefficient g	$3.8(2)\times10^{3}$	$4.2(1)\times10^{3}$
R-value	0.035	0.026
Weighted R-value	0.041	0.030

respectively for Ti–Ch and Ti–Cl. Full-ionized scattering factors were taken from Vol. III and IV of the *International Tables for X-ray Crystallography* for Mg^{2+}, Si^{4+}, Fe^{2+} and Ti^{4+} ions and from Tokonami (1965) for O^{2-} ions. The dispersion factors were also taken from the *International Tables*. After the convergence of isotropic refinements (R = 0.052 and 0.043 for chondrodite and clinohumite, respectively) with assumed random cation distributions in the octahedral sites, the site occupancy refinements were carried out as follows. Here we explain the procedure by taking Ti–Ch as example.

Initially, Mg, Fe′ (= Fe + Mn + Ni + Cr), and Ti were allotted to each of the three octahedral sites, and the occupancy factors of Mg and Fe′ in $M(1)$ and $M(2)$, which were chosen as the independent variables, were varied with the positional parameters, anisotropic thermal parameters, isotropic extinction parameter, and scale factor, with the octahedral site chemistries being constrained to agree with the chemical analyses. Then the site occupancy of Ti in $M(1)$ converged to a slightly negative value, assumed henceforth to be zero. Therefore, at the next stage, Ti was allotted only to $M(2)$ and $M(3)$ sites and the site occupancy factors of Mg in $M(1)$ and Mg and Fe′ in $M(2)$ were chosen as independent variables and refined together with the other parameters as described above. The same processes were repeated until all the variable site occupancies, independent or dependent, converged to non-negative value. The same method was used with Ti–Cl. The final weighted (unit weight) and unweighted values of R are 0.041 and 0.035 for Ti–Ch and 0.030 and 0.026 for Ti–Cl.

A difference Fourier map after refinement of Ti–Cl showed the hydrogen position approximately 1.02A from the O(9) site for OH. The peak height of the hydrogen atom is 0.5 e/A^3, and no other peak position with the peak height greater than 0.2 e/A^3 was observed within a sphere of radius 1.2A with its center at the O(9) site in the three-dimensional maps. A similar peak appeared in the same position in Ti–Ch, but could not be clearly distinguished from other ambiguous peaks.

Final atomic parameters are listed in Table 4. Interatomic distances, angles, and estimated standard errors were calculated using the ORFFE program of Busing *et al.* (1964). The results are given in Table 5. The observed and calculated structure factors are given in Table 6[3].

Discussion

The crystal structures of the humite-group minerals were recently refined by Gibbs and Ribbe (1969), Gibbs *et al.* (1970), Ribbe and Gibbs (1971), and Robinson *et al.* (1973). The structures of this series were originally described as consisting of alternating layers of olivine structure (Mg_2SiO_4) and of the $Mg(OH,F)_2$ composition. Ribbe *et al.* (1968), however, pointed out that such a description is misleading, and showed that the compositions of alternate layers should respectively be $Mg_2SiO_3(OH,F)$ and Mg(OH,F)O rather than the above compositions. Noting that Mg involved in the substitution scheme, Mg + 2(OH) $\rightleftarrows$ Ti + 2(O), is at $M(3)$, we have come to a view that the layers which contain OH should be so chosen that they concurrently contain $M(3)$. From such a viewpoint, we have found that the structures of the humite group can be looked upon as being composed of alternate layers whose compositions may well be expressed by $Mg_{2n-1}Si_nO_{4n-2}$ and 2Mg(OH,F)O; putting n = 1, 2, 3, and 4, we obtain compositions of norbergite, chondrodite, humite, and clinohumite respectively.

Mg, Fe, and Ti distributions

The distribution of Ti^{4+} may be considered as one of the major problems in the crystal chemistry of the humite mineral group. There are three distinct octahedral sites, $M(1)$, $M(2)$, and $M(3)$, in chondrodite and five sites, $M(1)_c$, $M(1)_n$, $M(2)_5$, $M(2)_6$, and $M(3)$, in clinohumite. Among these, the sites other than $M(3)$ in both structures belong to the layers of the olivine-type structure, the $M(3)$ site being in the Mg(OH)O layers. Our refinements indicate that Ti is almost completely concentrated in the $M(3)$ site

[3] To obtain a copy of this table, order Document AM-78-066 from the Business Office, Mineralogical Society of America, 1909 K Street, NW, Washington, DC 20006. Please remit $1.00 in advance for the microfiche.

Table 4. Atomic parameters of titanian chondrodite and clinohumite

Atom	Site occupancy	X	Y	Z	Beq.*	β_{11}	β_{22}	β_{33}	β_{12}	β_{13}	β_{23}
				Ti-Chondrodite							
M(1)	0.91(1)Mg 0.09(1)Fe'	0.5	0.0	0.5	0.45(2)	462(42)	121(10)	173(16)	-4(16)	44(21)	4(9)
M(2)	0.87(5)Mg 0.12(6)Fe' 0.01(8)Ti	0.01538(19)	0.17316(8)	0.30648(10)	0.52(4)	623(78)	119(18)	238(31)	15(11)	-5(15)	52(10)
M(3)	0.66(5)Mg 0.13(6)Fe' 0.21(8)Ti	0.49525(16)	0.89343(7)	0.07466(9)	0.74(4)	600(62)	241(15)	243(25)	81(10)	-91(13)	-26(8)
Si		0.07499(16)	0.14380(7)	0.70431(10)	0.39(1)	351(23)	109(5)	179(9)	-14(9)	-16(12)	33(5)
O(1)		0.77728(41)	0.00071(18)	0.29554(25)	0.47(3)	493(58)	103(13)	247(23)	-31(24)	37(32)	47(14)
O(2)		0.72461(43)	0.24271(18)	0.12284(25)	0.56(4)	567(62)	125(13)	244(24)	10(25)	8(33)	-13(15)
O(3)		0.22378(41)	0.16998(18)	0.53152(24)	0.49(4)	504(61)	158(14)	200(24)	23(25)	59(31)	76(15)
O(4)		0.26619(39)	0.85625(19)	0.29560(26)	0.48(3)	339(59)	156(14)	256(24)	-15(25)	6(33)	74(15)
(OH,O)		0.25658(45)	0.05534(20)	0.09607(27)	0.85(4)	991(80)	210(15)	316(26)	-0(29)	158(38)	9(17)
				Ti-Clinohumite							
$M(1)_c$	0.88(9)Mg 0.10(10)Fe' 0.02(13)Ti	0.5	0.0	0.5	0.47(6)	428(119)	144(26)	64(15)	-11(16)	-8(12)	24(6)
$M(1)_n$	0.87(5)Mg 0.11(6)Fe' 0.02(6)Ti	0.49665(18)	0.94603(7)	0.27464(5)	0.50(4)	500(72)	140(16)	61(9)	13(10)	29(7)	0(4)
$M(2)_5$	0.87(1)Mg 0.13(1)Fe'	0.01510(17)	0.13976(7)	0.16975(5)	0.52(2)	621(31)	119(6)	70(4)	-6(11)	-3(8)	19(3)
$M(2)_6$	0.87(1)Mg 0.13(1)Fe'	0.51051(18)	0.25040(7)	0.38777(5)	0.48(2)	618(31)	98(6)	67(4)	-13(10)	-18(8)	9(3)
M(3)	0.67(10)Mg 0.15(12)Fe' 0.18(16)Ti	0.49488(15)	0.88433(6)	0.04094(5)	0.75(3)	631(62)	249(14)	77(8)	109(10)	-41(7)	-23(3)
Si(1)		0.07266(14)	0.06676(6)	0.38979(5)	0.39(1)	316(26)	106(5)	64(3)	-11(9)	-5(7)	15(3)
Si(2)		0.07556(14)	0.17647(6)	0.83515(5)	0.40(1)	390(26)	107(5)	55(3)	9(9)	3(7)	14(3)
O(1,1)		0.73273(41)	0.06454(17)	0.38817(13)	0.50(4)	421(72)	148(14)	69(8)	13(25)	24(19)	16(9)
O(1,2)		0.28065(39)	0.42061(16)	0.38784(13)	0.48(3)	570(68)	112(13)	68(8)	9(24)	16(19)	22(8)
O(1,3)		0.22140(40)	0.11282(17)	0.29420(13)	0.52(4)	524(71)	130(13)	79(8)	-7(25)	-10(19)	32(8)
O(1,4)		0.22022(39)	0.15850(17)	0.48640(13)	0.52(3)	482(67)	145(14)	66(8)	15(25)	-1(19)	-11(8)
O(2,1)		0.23521(41)	0.32327(17)	0.16313(13)	0.48(4)	489(72)	137(14)	64(8)	8(25)	2(19)	22(8)
O(2,2)		0.77724(39)	0.96806(16)	0.16339(13)	0.47(3)	537(69)	98(13)	73(8)	39(24)	16(19)	13(8)
O(2,3)		0.72257(41)	0.27891(17)	0.26139(14)	0.54(4)	599(73)	149(14)	69(8)	4(25)	-32(19)	36(8)
O(2,4)		0.72554(41)	0.22876(17)	0.06896(13)	0.59(4)	720(72)	138(14)	70(8)	-21(25)	51(20)	-2(8)
O(9)≡(OH,O)		0.25717(45)	0.04469(18)	0.05356(14)	0.87(4)	1123(83)	222(15)	87(9)	14(28)	116(22)	1(9)
H		0.06**	0.022	0.027							

* *Equivalent isotropic temperature factor, calculated from anisotropic ones(Hamilton, 1959).*

** *Determined from the three-dimensional difference Fourier map.*

Anisotropic temperature factors($X10^5$) are of the form: $\exp\{-\sum_{i=1}^{3}\sum_{j=1}^{3} h_i h_j \beta_{ij}\}$.

Fe'=Fe+Mn+Ni+Cr

The error in the final figure is indicated in parentheses.

(Table 4), and clearly explain the fact that the Ti/Si ratio in Ti–Ch is always just twice as great as that in Ti–Cl.

As to Mg–Fe distributions, Fe/Mg ratio is higher in the $M(3)$ site than in the other sites in both minerals. This conforms with the result of Robinson *et al.* (1973) that $M(3)$ in Ti–Cl is relatively enriched in Fe, in contrast to Ti-free clinohumite and humite, where Fe is enriched in the other sites. This trend is consistent with the observation that the total Fe/Mg ratio increases in the order of olivine, Ti–Cl, and Ti–Ch, *i.e.*, in increasing order of Mg(OH)O layers in the crystals, when these minerals coexist (McGetchin *et al.*, 1970; Aoki *et al.*, 1976).

Hydrogen position and structure stability

Bond-length variations in the cation octahedra agree with the above-mentioned Ti occupancy. Figure 2 shows variations of mean octahedral M–O bond lengths and shared and unshared (OH,O)–(OH,O) distances with O_{Ti} content [O_{Ti} is the oxygen content which substitutes for OH in the following scheme, Mg + 2(OH) $\rightleftarrows$ Ti + 2(O)]. In Figure 2, mean $M(1)$–O and mean $M(2)$–O remains nearly constant with O_{Ti} content, whereas mean $M(3)$–O clearly decreases with O_{Ti} content corresponding to Ti concentration in $M(3)$ sites.

The occurrence of the substitution scheme, Mg + 2(OH) $\rightleftarrows$ Ti + 2(O), in the Mg(OH)O layers is closely related to the hydrogen locations of the OH groups. The locations of hydrogen atoms of Ti–Cl are depicted in Figure 3, which shows a portion of the final difference Fourier section, $x = 0.06$, passing through the hydrogen position, H, together with octahedra formed by neighboring oxygen atoms. This figure also shows the corresponding atomic configuration as

Table 5. Interatomic bond distances, angles, and estimated standard errors for titanian chondrodite and clinohumite

Ti-Chondrodite

Si tetrahedron, SiO_4		
Si-O(4)	1.613(2)Å	
-O(2)	1.637(2)	
-O(3)	1.637(2)	
-O(1)	1.647(2)	
mean	1.634	
		Angle at Si
O(1)-O(3)	2.562(3) *t*	102.6°
O(1)-O(2)	2.558(3) *t*	102.3
O(2)-O(3)	2.578(3) *t*	103.9
O(1)-O(4)	2.750(3)	115.1
O(2)-O(4)	2.750(3)	115.6
O(3)-O(4)	2.748(3)	115.5
mean	2.658	109.2

M(1) octahedron, MO_6		
M(1)-O(1) [2]	2.083(2)	
-O(3) [2]	2.134(2)	
-O(4) [2]	2.109(2)	
mean	2.109	
		Angle at M
O(1)-O(3) [2]	2.562(3) *t*	74.8
O(3)-O(4) [2]	2.828(3) *o*	83.6
O(1)-O(4) [2]	2.839(3) *o*	85.3
O(1)-O(4)' [2]	3.084(3)	94.7
O(3)-O(4)' [2]	3.162(3)	96.4
O(1)-O(3)' [2]	3.349(3)	105.2
mean	2.968	90.0

M(2) octahedron, $MO_5(OH,O)$		
M(2) -O(3)	2.043(2)Å	
-O(1)	2.083(2)	
-O(4)	2.179(2)	
-O(3)'	2.180(2)	
-O(2)	2.281(2)	
-(OH,O)	2.051(2)	
mean	2.136	
		Angle at M
O(2)-O(3)'	2.578(3) *t*	70.4°
O(2)-O(4)	2.824(3) *o*	78.5
O(3)'-O(4)	2.828(3) *o*	80.7
O(1)-O(3)	2.971(3)	92.1
O(3)-O(3)'	3.018(2)	90.9
O(3)-O(4)	3.090(3)	94.0
O(1)-O(2)	3.228(3)	95.3
O(1)-O(3)'	3.225(3)	98.1
(OH,O)-O(1)	2.920(3)	89.9
(OH,O)-O(4)	2.983(3)	89.6
(OH,O)-O(2)	3.136(3)	92.6
(OH,O)-O(3)	3.252(3)	105.2
mean	3.004	89.8

M(3) octahedron, $MO_4(OH,O)_2$		
M(3)-O(2)	2.010(2)Å	
-O(4)	2.194(2)	
-O(2)'	2.170(2)	
-O(1)	2.185(2)	
-(OH,O)	1.976(2)	
-(OH,O)'	1.987(2)	
mean	2.087	
		Angle at M
O(1)-O(2)'	2.558(3) *t*	72.0°
O(2)'-O(4)	2.824(3) *o*	80.6
O(1)-O(4)	2.839(3) *o*	80.8
(OH,O)'-(OH,O)	2.786(4) *o*	89.3
(OH,O)'-O(2)	2.899(3)	93.0
(OH,O)-O(4)	2.976(3)	90.9
(OH,O)'-O(1)	2.960(3)	90.2
(OH,O)-O(2)	2.989(3)	97.2
(OH,O)-O(1)	3.074(3)	95.1
(OH,O)'-O(2)'	3.122(3)	97.2
O(2)-O(4)	3.123(3)	95.8
O(2)'-O(2)	3.094(3)	95.4
mean	2.937	89.8

Ti-Clinohumite

Si(1) tetrahedron, SiO_4		
Si(1)-O(1,1)	1.613(2)Å	
-O(1,2)	1.652(2)	
-O(1,3)	1.635(2)	
-O(1,4)	1.630(2)	
mean	1.633	
		Angle at Si
O(1,1)-O(1,2)	2.742(3)	114.2°
O(1,1)-O(1,3)	2.743(3)	115.2
O(1,1)-O(1,4)	2.756(3)	116.4
O(1,2)-O(1,3)	2.553(2) *t*	101.9
O(1,2)-O(1,4)	2.559(2) *t*	102.5
O(1,3)-O(1,4)	2.585(3) *t*	104.7
mean	2.656	109.2

Si(2) tetrahedron, SiO_4		
Si(2)-O(2,1)	1.615(2)	
-O(2,2)	1.646(2)	
-O(2,3)	1.636(2)	
-O(2,4)	1.641(2)	
mean	1.635	
		Angle at Si
O(2,1)-O(2,2)	2.751(3)	115.0
O(2,1)-O(2,3)	2.757(3)	116.0
O(2,1)-O(2,4)	2.746(3)	115.0
O(2,2)-O(2,3)	2.565(2) *t*	102.8
O(2,2)-O(2,4)	2.552(2) *t*	101.9
O(2,3)-O(2,4)	2.588(2) *t*	104.3
mean	2.660	109.2

$M(1)_c$ octahedron, MO_6		
$M(1)_c$-O(1,1) [2]	2.096(2)Å	
-O(1,2) [2]	2.079(2)	
-O(1,4) [2]	2.138(2)	
mean	2.104	
		Angle at M
O(1,2)-O(1,4) [2]	2.559(2) *t*	74.7°
O(1,1)-O(1,2) [2]	2.850(3) *o*	86.1
O(1,4)-O(1,1) [2]	2.857(3) *o*	84.9
O(1,2)-O(1,1) [2]	3.051(3)	93.9
O(1,1)-O(1,4) [2]	3.125(2)	95.1
O(1,2)-O(1,4) [2]	3.352(3)	105.3
mean	2.966	90.0

$M(1)_n$ octahedron, MO_6		
$M(1)_n$-O(1,1)	2.106(2)	
-O(1,2)	2.088(2)	
-O(1,3)	2.132(2)	
-O(2,1)	2.098(2)	
-O(2,2)	2.068(2)	
-O(2,3)	2.155(2)	
mean	2.108	
		Angle at M
O(2,2)-O(2,3)	2.565(3) *t*	74.8
O(1,2)-O(1,3)	2.553(2) *t*	74.5
O(1,1)-O(1,3)	2.834(3) *o*	84.0
O(1,2)-O(1,1)	2.850(3) *o*	85.6
O(2,2)-O(2,1)	2.851(3) *o*	86.3
O(2,1)-O(2,3)	2.858(3) *o*	84.5
O(2,3)-O(1,1)	3.121(2)Å	94.2°
O(1,1)-O(2,2)	3.057(3)	94.2
O(2,1)-O(1,2)	3.057(3)	93.8
O(1,3)-O(2,1)	3.177(2)	97.4
O(2,3)-O(1,2)	3.342(3)	104.0
O(1,3)-O(2,2)	3.371(2)	106.8
mean	2.970	90.0

$M(2)_6$ octahedron, MO_6		
$M(2)_6$-O(1,2)	2.062(2)	
-O(2,3)	2.071(2)	
-O(1,1)	2.184(2)	
-O(1,3)	2.199(2)	
-O(1,4)	2.055(2)	
-O(1,4)'	2.259(2)	
mean	2.138	
		Angle at M
O(1,3)-O(1,4)'	2.585(3) *t*	70.9
O(1,3)-O(1,1)	2.834(3) *o*	80.6
O(1,1)-O(1,4)'	2.857(3) *o*	80.0
O(1,1)-O(1,4)	3.033(2)	91.3
O(1,4)-O(2,3)	3.392(3)	110.6
O(2,3)-O(1,1)	3.056(2)	91.8
O(1,4)'-O(1,2)	3.249(2)	97.4
O(1,2)-O(1,3)	3.193(2)	97.0
O(1,4)'-O(1,4)	3.007(2)	88.2
O(1,4)-O(1,2)	2.918(3)	90.3
O(1,2)-O(2,3)	2.925(3)	90.1
O(2,3)-O(1,3)	3.011(3)	89.6
mean	3.005	89.8

t = edge shared between tetrahedron and octahedron.
o = edge shared between two octahedra.
Superscript prime distinguishes two similar anions in the same polyhedron.
[2] indicates multiplicity factor for bonds in centrosymmetric octahedron.
The error in the final figure is indicated in parentheses.
Estimated standard error of all angles is 0.1°.

Table 5. (continued)

Ti-Clinohumite

$M(2)_5$ octahedron, $MO_5(OH,O)$		
$M(2)_5$-O(1,3)	2.030(2)Å	
-O(2,2)	2.083(2)	
-O(2,3)	2.206(2)	
-O(2,4)	2.261(2)	
-O(2,1)	2.174(2)	
-(OH,O)	2.053(2)	
mean	2.135	
		Angle at M
O(2,3)-O(2,4)	2.588(2)*t*	70.8°
O(2,4)-O(2,1)	2.825(3)*o*	79.1
O(2,3)-O(2,1)	2.858(3)*o*	81.5
O(1,3)-O(2,1)	3.065(2)	93.6
O(2,4)-O(2,2)	3.200(2)	94.8
O(2,2)-O(2,3)	3.233(2)	97.8
O(2,2)-O(1,3)	2.975(3)Å	92.6°
O(1,3)-O(2,3)	3.002(3)	90.2
(OH,O)-O(2,2)	2.919(3)	89.8
(OH,O)-O(2,1)	2.971(3)	89.3
(OH,O)-O(1,3)	3.241(3)	105.1
(OH,O)-O(2,4)	3.136(3)	93.1
mean	3.001	89.8
$M(3)$ octahedron, $MO_4(OH,O)_2$		
M(3)-O(2,4)'	2.011(2)	
-O(2,4)	2.168(2)	
-O(2,2)	2.191(2)	
-O(2,1)	2.188(2)	
-(OH,O)'	1.988(2)	
-(OH,O)	1.978(2)	
mean	2.087	
		Angle at M
O(2,4)-O(2,2)	2.552(3)Å*t*	71.7°
O(2,4)-O(2,1)	2.825(3)*o*	80.8
O(2,1)-O(2,2)	2.851(3)*o*	81.2
(OH,O)'-(OH,O)	2.792(4)*o*	89.5
(OH,O)'-O(2,2)	2.954(3)	89.8
(OH,O)'-O(2,4)	3.124(3)	97.4
(OH,O)'-O(2,4)'	2.901(3)	93.0
(OH,O)-O(2,4)'	2.988(3)	97.0
(OH,O)-O(2,2)	3.070(3)	94.7
(OH,O)-O(2,1)	2.957(2)	90.3
O(2,4)'-O(2,1)	3.122(3)	96.0
O(2,4)'-O(2,4)	3.115(3)	96.3
mean	2.938	89.8

viewed along an axis perpendicular to the plane defined by [100] and an axis passing through O(9) and O(9)′. Since the occupancy factor of hydrogen in the present case is 0.57, when one of the centrosymmetric pair of hydrogen positions, H and H′, is occupied by a hydrogen atom, the other position should be almost vacant. If, however, the numbers of OH per cell were increased to give an extreme case such as that, for example, in the OH end-member of clinohumite, the paired positions, H and H′, would be fully occupied by hydrogen atoms, giving rise to a strong repulsion between them. Such a structure would be less stable. This situation may be rephrased in a reverse way: suppose that the degree of substitution, Mg + 2(OH) → Ti + 2(O), is increased in the OH end-member, and reaches the state that half of the OH groups involved in the substitution scheme are replaced by oxygen atoms (as is nearly the case in this study), then the hydrogen–hydrogen repulsion in the structure will vanish and the structure will become more stable.

An inspection of interatomic distances appears to support this view. Among twelve distances between OH and its twelve anion neighbors, the unshared (OH,O)–(OH,O) distance in Ti–Ch is shorter by 0.17A compared to that in the end-member OH–chondrodite (Fig. 2), while the other eleven (OH,O)–(OH,O) or –O distances are nearly constant or only decrease by at most 0.12A. The observed instability at atmospheric pressure of OH end-members of the humite-group minerals may thus be explained in terms of the hydrogen–hydrogen repulsion.

Regarding hydrogen positions, Yamamoto (1977) reported, based on X-ray analysis, a set of three possible orientations for the OH dipole in the OH end-member of chondrodite synthesized under high pressure, the dipole being statistically oriented among the three directions. One of those orientations is similar to our result. To confirm other orientations, further study would probably be required.

So far as our specimens are concerned, the maximum content of TiO_2 in chondrodite is 10.19 weight percent and in clinohumite 5.7 weight percent. The two values correspond to about a quarter of Ti occupancy in the $M(3)$ sites of Mg(OH)O layers in respective structures. Noting that these minerals coexisted with ilmenite, we may assume that further substitution of Ti for Mg would not take place, and the above-mentioned TiO_2 contents are nearly maximum values for naturally occurring chondrodite and clinohumite respectively. Since the substitution of Ti for Mg is linked with that of O for OH, $M(3)$ is the most favorable site to accommodate Ti from the viewpoint of the Pauling's electrostatic valence rule. Nevertheless, the substitution by itself still gives rise to a local disturbance of the valence rule and, when the Ti content exceeds the observed maximum value, the structure would become significantly unstable. The above-mentioned limited Ti substitution may be explained along this line.

Summary and conclusions

Almost complete Ti ordering in Mg(OH)O layers of the structures of chondrodite and clinohumite was ascertained in the present work. This explains why chondrodite accommodates more Ti than clinohumite, contrary to suggestions in previous reports.

The hydrogen locations are such that they give rise to a strong H–H repulsion in Mg(OH)O layers. It follows that the replacement, to a certain extent, of OH by O, as in the scheme Mg + 2(OH) → Ti +2(O), or replacement of OH by F would stabilize the structure; the two substitution schemes, Mg + 2(OH) → Ti + 2(O) and OH → F, appear to play a similar role in

stabilizing the structure. Thus under a fluorine-free condition, hydroxyl–chondrodite and –clinohumite appear to be stabilized through incorporation of Ti in place of Mg.

The present study, as well as experiments under high pressure and temperature, shows that only two monoclinic phases, among four known members of the humite group, are stable under high-pressure conditions.

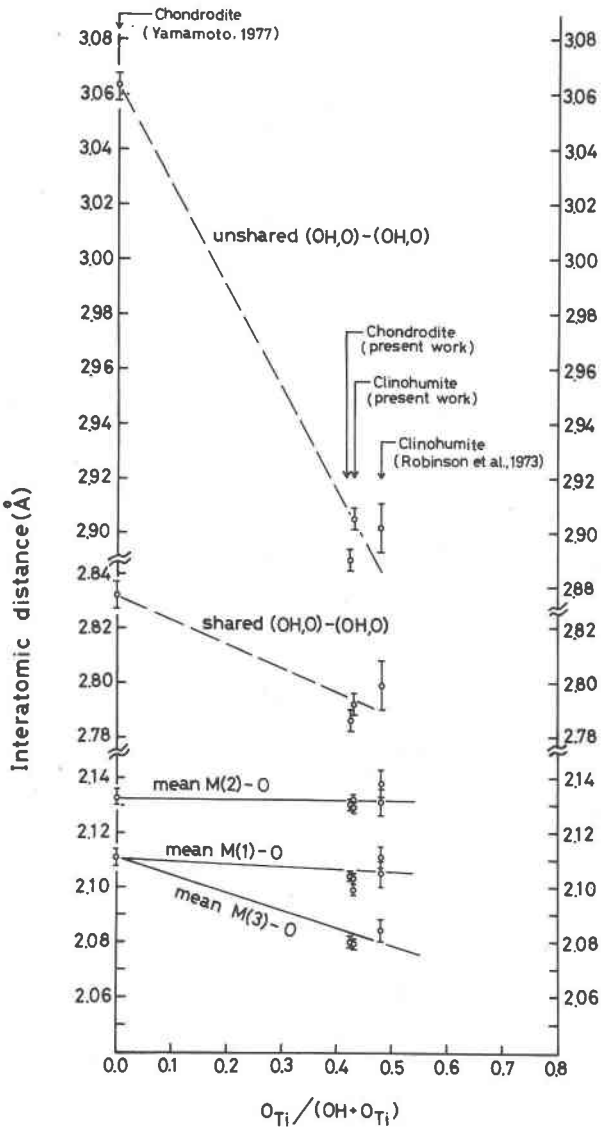

Fig. 2. Variations of mean octahedral M–O, shared and unshared (OH,O)–(OH,O) distances with O_{Ti} content [Mg + 2(OH) $\rightleftarrows$ Ti + 2(O_{Ti})]. For clinohumite, mean $M(1)_c$–O and $M(1)_n$–O, likewise mean $M(2)_5$–O and $M(2)_6$–O, are plotted separately. Mean M–O distances are corrected for Fe content present in each site by a reduction of 0.05A multiplied by the occupancy factor of Fe in each site [0.05A = $r_{Fe^{2+}} - r_{Mg^{2+}} = 0.77 - 0.72$A, where $r_{Fe^{2+}}$ are ionic radii of Fe^{2+} and Mg^{2+}(Shannon and Prewitt, 1969)].

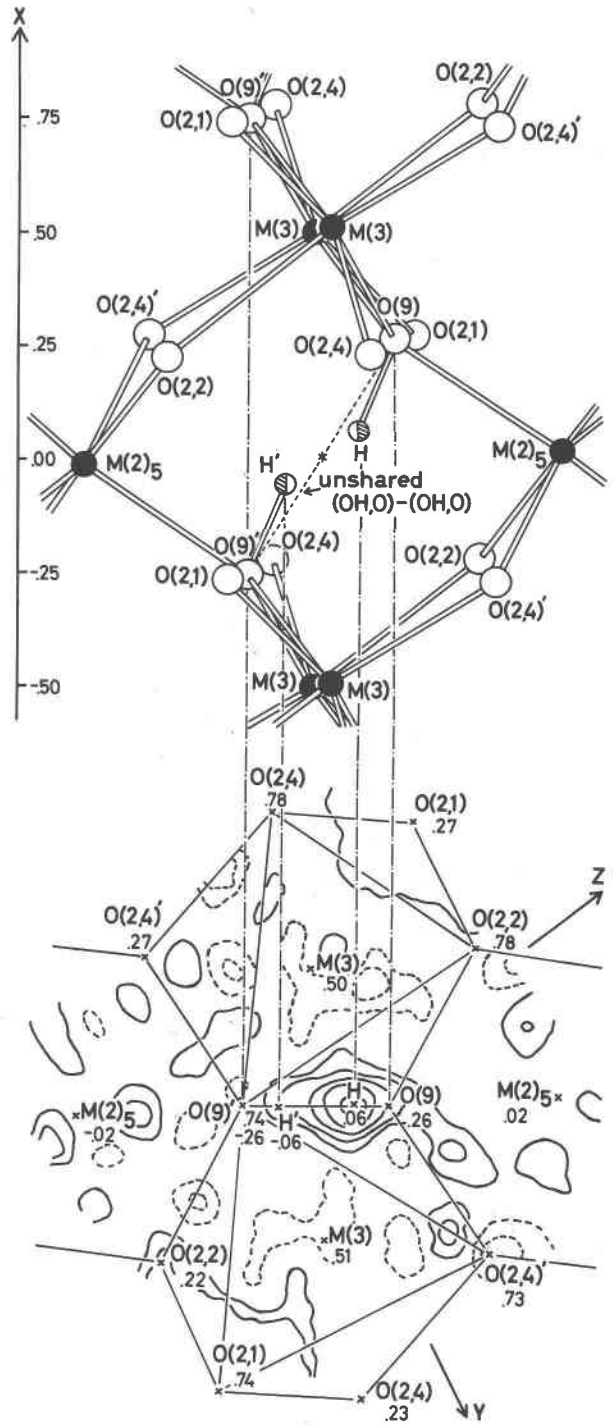

Fig. 3. Lower figure: portion of the difference Fourier section, x = 0.06, of titanian clinohumite, passing through the hydrogen position, H; neighboring octahedra formed by oxygen atoms are indicated. Contours are drawn at an interval of 0.1 e/A^3, zero contours being omitted, and negative contours broken. Numbers give fractional atomic coordinates along a.

Upper figure: corresponding atomic configuration viewed along an axis perpendicular to the plane as defined by [100] and an axis passing through O(9) and O(9)'. Inversion center is indicated by *.

The occurences of the fluorine-free Ti-Ch and Ti-Cl reported so far are limited to kimberlite, while those of Ti-free fluor-humite group minerals are almost all in metamorphosed and metasomatised limestones and dolomites adjacent to acid plutonic rocks. Comparing these facts with the high-pressure experiments by Yamamoto and Akimoto (1974, 1977), it appears that the partial substitution of TiO_2 for $Mg(OH)_2$ does not significantly affect the stability field of chondrodite and clinohumite, although there remains a possibility that the lower pressure limit of the stability field may be lowered by the stabilization of the structures with the above-mentioned substitution. Further experimental studies to confirm this point would probably be worthwhile as a contribution to mantle mineralogy.

Acknowledgments

We thank Professor K. Aoki, Tohoku University, for kindly placing his kimberlite specimens at our disposal and for discussion, Professor S. Akimoto, University of Tokyo, for discussion about high-pressure and high-temperature experiments, and Mr. M. Akaogi, University of Tokyo, for providing us with his microprobe data and discussion. Thanks are also due to Dr. K. Yamamoto, Nagoya University, for sending information about his results prior to publication. Computations were carried out on HITAC 8700/8800 at the Computer Center of the University of Tokyo.

References

Aoki, K., K. Fujino and M. Akaogi (1976) Titanochondrodite and titanoclinohumite derived from the upper mantle in the Buell Park kimberlite, Arizona, U.S.A. *Contrib. Mineral. Petrol., 56,* 243–253.

Busing, W. R., K. O. Martin and H. A. Levy (1964) ORFFE, a Fortran crystallographic function and error program. *U. S. Nat. Tech. Inf. Serv. ORNL-TM-306.*

Coppens, H. and W. C. Hamilton (1970) Anisotropic extinction corrections in the Zachariasen approximation. *Acta Crystallogr., A26,* 71–83.

Gibbs, G. V. and P. H. Ribbe (1969) The crystal structures of the humite minerals: I. Norbergite. *Am. Mineral., 54,* 376–390.

———, ——— and C. P. Anderson (1970) The crystal structures of the humite minerals: II. Chondrodite. *Am. Mineral., 55,* 1182–1194.

Hamilton, W. C. (1959) On the isotropic temperature factor equivalent to a given anisotropic temperature factor. *Acta Crystallogr., 12,* 609–610.

Jones, N. W. (1969) Crystallographic nomenclature and twinning in the humite minerals. *Am. Mineral., 54,* 309–313.

———, P. H. Ribbe and G. V. Gibbs (1969) Crystal chemistry of the humite minerals. *Am. Mineral., 54,* 391–411.

Kocman, V. and J. Rucklidge (1973) The crystal structure of a titaniferous clinohumite. *Can. Mineral., 12,* 39–45.

McGetchin, T. R., L. T. Silver and A. A. Chodos (1970) Titanoclinohumite: A possible mineralogical site for water in the upper mantle. *J. Geophys. Res., 75,* 255–259.

Ribbe, P. H., G. V. Gibbs and N. W. Jones (1968) Cation and anion substitutions in the humite minerals. *Mineral. Mag., 37,* 966–975.

——— and ——— (1971) Crystal structures of the humite minerals: III. Mg/Fe ordering in humite and its relation to other ferromagnesian silicates. *Am. Mineral., 56,* 1155–1173.

Robinson, K., G. V. Gibbs and P. H. Ribbe (1973) The crystal structures of the humite minerals: IV. Clinohumite and titanoclinohumite. *Am. Mineral., 58,* 43–49.

Shannon, R. D. and C. T. Prewitt (1969) Effective ionic radii in oxides and fluorides. *Acta Crystallogr., B25,* 925–946.

Tokonami, M. (1965) Atomic scattering factor for O^{2-}. *Acta Crystallogr., 19,* 486.

Yamamoto, K. (1977) Hydroxyl-chondrodite. *Acta Crystallogr., B33,* 1481–1485.

——— and S. Akimoto (1974) High pressure and high temperature investigations in the system MgO–SiO_2–H_2O. *J. Solid State Chem., 9,* 187–195.

——— and ——— (1977) The system MgO–H_2O–SiO_2 at high pressures and temperatures—Stability field for hydroxyl-chondrodite, hydroxyl-clinohumite and 10 A-phase. *Am. J. Sci., 277,* 288–312.

Manuscript received March 4, 1977; accepted for publication November 28, 1977.